

# Why is the cloud albedo - particle size relationship different in optically thick and optically thin clouds?

Ulrike Lohmann,<sup>1</sup> George Tselioudis,<sup>2</sup> and Chris Tyler<sup>1</sup>

**Abstract.** Recent studies have analyzed satellite data in terms of the relationship of cloud albedo with droplet size for warm clouds. It was found that for optically thick marine clouds ( $\tau > 15$ ) the cloud albedo increases with decreasing cloud droplet effective radius ( $r_e$ ). For optically thinner marine clouds ( $\tau < 15$ ) cloud albedo increases with increasing  $r_e$  as to be expected if the liquid water content is adiabatic. Hypotheses for the change in sign in the  $\tau - r_e$  relationship are deviations from an adiabatic liquid water content or the presence of single layer versus multi layer clouds. In this study, the ECHAM model, which exhibits this sign change in the  $\tau - r_e$  correlation for optically thin and thick marine clouds, is used to test these hypotheses. Probability density functions of  $\tau - r_e$  show that the change in sign of the correlation can be attributed to precipitating versus non-precipitating clouds, but not to the difference in single layer versus multi-layer clouds.

## 1. Introduction

The indirect aerosol effect, whereby anthropogenic aerosols change cloud optical properties (cloud albedo effect), is often calculated assuming a constant liquid water content, [e.g. Jones *et al.*, 1994; Boucher and Lohmann, 1995]. Then an increase in aerosols leads to an increase in cloud droplet number concentration with smaller cloud droplet effective radii and, thus, a higher cloud optical depth. The assumption of a constant liquid water path (LWP) is justified by observational evidence from 4 field studies over Canada and the United States [Leaith *et al.*, 1992]. Different conclusions came out of ship track studies [e.g. King *et al.*, 1993] and from MCR (multi-spectral radiometer measurements) studies during the First International Satellite Cloud Climatology Project (ISCCP) Regional Experiment (FIRE) off the coast of California [Nakajima *et al.*, 1991] where LWP was higher in the polluted case due to the absence of drizzle size drops. Brenquier *et al.*, [1999, 2000] analyzed data obtained from the Second Aerosol Characterization Experiment (ACE2) in the Atlantic and found evidence

for the indirect cloud albedo effect on the scale of a cloud system by comparing a clean cloud with a polluted cloud. For a given geometrical thickness of the cloud, the reflectances at 754 nm and 1535 nm are higher in the polluted case than in the clear case, even though the mean LWP is lower in the polluted case.

The relationship of cloud albedo and LWP with droplet size was studied on a global scale using ISCCP data [Han *et al.*, 1998]. They find that only for optically thick clouds ( $\tau > 15$ ) and for clouds over land does the cloud albedo (and optical depth) increase with decreasing droplet size. That can be understood from the following expression for  $\tau$ :

$$\tau = \frac{3}{2} \frac{\text{LWC } \Delta z}{r_e} \quad (1)$$

where LWC = liquid water content (g/m<sup>3</sup>),  $\Delta z$  cloud thickness, and  $r_e$  = effective cloud droplet radius:  $\int_0^\infty r^3 n(r) dr / \int_0^\infty r^2 n(r) dr$ . If LWC and  $\Delta z$  are constant, then  $\tau$  varies with  $1/r_e$ .

For optically thinner clouds ( $\tau < 15$ ) LWP and cloud albedo increase with increasing  $r_e$  as to be expected in the droplet growth state where the cloud droplet number concentration ( $N_l$ ) is almost constant. It can be understood if the equation for  $r_e$ :

$$r_e \sim \sqrt[3]{\frac{3 \text{LWC}}{4 \pi \rho_l N_l}} \quad (2)$$

where  $\rho_l$  is the water density, is used to replace LWC with  $N_l$  in (1):

$$\tau \sim r_e^2 N_l \Delta z \quad (3)$$

i. e. if  $N_l$  and  $\Delta z$  are constant, then  $\tau$  varies with  $r_e^2$ . If the cloud is assumed to be adiabatic, then LWC is proportional to  $\Delta z$  such that

$$\tau \sim r_e^5 N_l^2 \quad (4)$$

Austin *et al.*, [1999] analyzed data from the Advanced Very High Resolution Radiometer (AVHRR) off the coast of California. They identified different types of scenes in terms of probability density functions of  $\tau$  and  $r_e$ . The satellite-retrieved plots of  $\tau$  and  $r_e$  show that  $r_e \sim \tau^{1/5}$ . This relationship is consistent with little variability in the quantity ( $N_l/c_{adia}$ ), where  $c_{adia}$  is a measure of how close LWP is to it's adiabatic value. In particular, if  $c_{adia}=1$  then the layer is adiabatic and  $r_e \sim \tau^{1/5}$  implies little variability in  $N_l$  in the scene.

It has been suggested that the  $\tau - r_e$  anticorrelation, on the other hand, is caused by water loss due to precipitation [Nakajima and Nakajima, 1995] or that it is a result of analyzing multi-layer clouds where the effective radius measured at cloud top does not correspond to the integrated  $\tau$  over all cloud layers [Schüller, 1999].

We test both hypotheses using the ECHAM general circulation model (GCM) which is able to reproduce the change

<sup>1</sup>Dept. of Physics, Dalhousie University, Halifax, Canada.

<sup>2</sup>NASA/GISS, New York, N.Y., U.S.A.

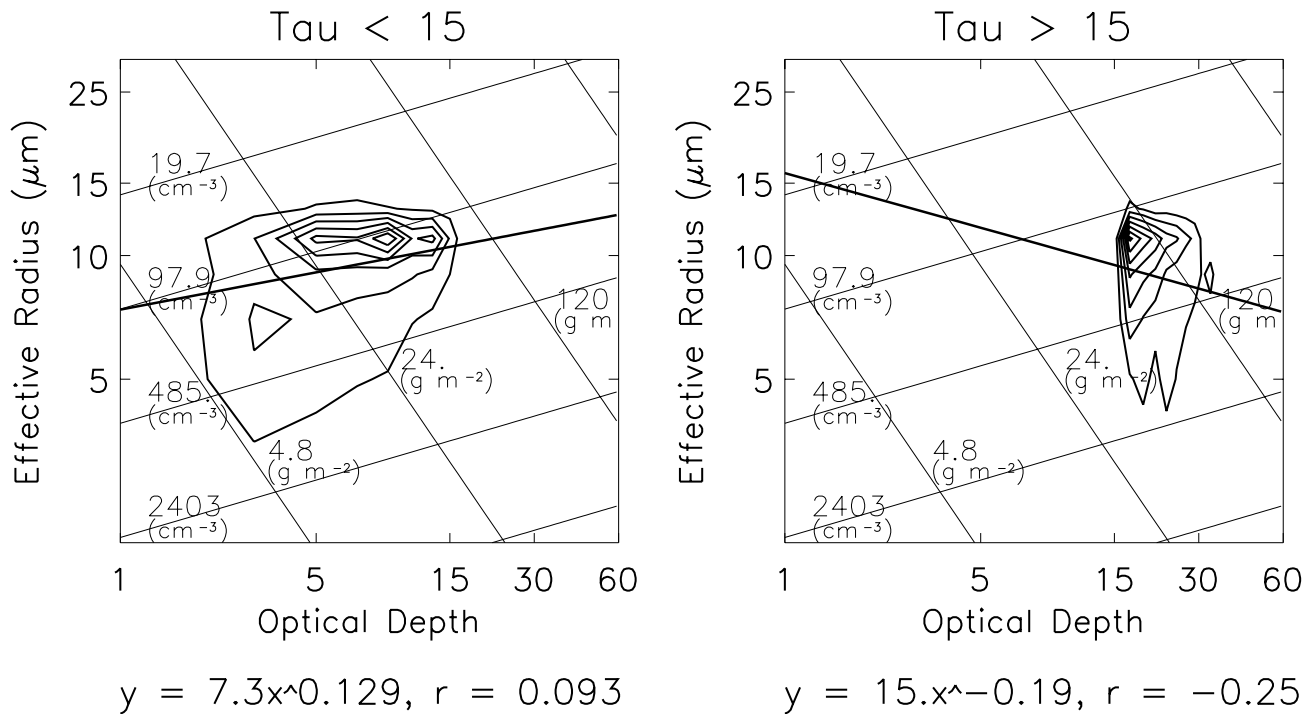


**Figure 1.** Log-log contour plots of  $r_e$  and  $\tau$  off the coast of California for clouds with  $\tau < 15$  (left) and  $\tau > 15$  (right). Thin lines going from the lower left to the upper right are lines of constant  $N_l$  and those going from the upper left to the lower right are lines of constant LWP (following Austin *et al.*, [1999]). The regression equation is the best least square fit through the data and  $r$  is the correlation coefficient.

in correlation of  $\tau$  with  $r_e$  for optically thin and thick warm clouds ( $T > 273.2\text{K}$ ) over the oceans on a global scale [Lohmann *et al.*, 1999]. In this ECHAM version, the independent variables are  $N_l$  and LWC, which are solved for prognostically. Cloud droplet activation depends on updraft velocity and number of aerosols, whereas the condensation rate is calculated using a saturation adjustment scheme. Both variables are depleted by precipitation formation, evaporation, accretion with rain and snow and freezing.

$\tau$  is calculated similarly to (1) but as a fit to match Mie calculations results for the model's solar bands [Rockel *et al.*, 1991].  $r_e$  is taken at cloud top calculated according to (2) to mimic the satellite view as close as possible. We use data twice daily from one year from the ECHAM GCM run in T30 resolution (approximately  $3.75^\circ$  by  $3.75^\circ$ ) in a region off the coast of California ( $24^\circ\text{N}$  to  $35^\circ\text{N}$ ,  $150^\circ\text{W}$  to  $136^\circ\text{W}$ ) which encompasses the scenes analyzed in Austin *et al.* [1999].

## Results

Figure 1 shows the probability density function of  $\tau$  and  $r_e$  off the coast of California for optically thin ( $\tau < 15$ ) and optically thick clouds ( $\tau > 15$ ). For the optically thin clouds, LWP and  $\tau$  increase as the effective radius increases. The exponent in the regression of  $r_e$  and  $\tau$  is 0.13, which is close to the value expected for an adiabatic cloud (0.2) in which  $N_l$  is constant.

For optical thick clouds, the slope is -0.19, which is in between the slope to be expected for a constant LWP (-1) and constant  $N_l$ . The correlation coefficients for those two cases match what is found globally from ISCCP data [Han *et al.*, 1998] and from ECHAM [Lohmann *et al.*, 1999].

A slope closer to that expected for an adiabatic cloud with constant  $N_l$  was found from AVHRR data off the Californian coast [Austin *et al.*, 1999]. They obtained slopes of 0.19 to 0.2 in at least 4 scenes. However, one has to bear in mind that the scenes from AVHRR are comprised of individual pixels, which are much smaller than the size of a grid box in ECHAM, so that a more uniform picture can be expected from the satellite data.

Austin *et al.*, [1999] also evaluated four scenes of thicker cloud layers, defined as those where the mean LWP exceeded  $100\text{ g m}^{-2}$ . In only one of these 4 scenes did they find a decrease in effective radius with increasing optical depth. Following their analysis, we sorted the ECHAM data into grid boxes in which  $\text{LWP} > 100\text{ g m}^{-2}$  and those where  $\text{LWP} < 100\text{ g m}^{-2}$  (not shown). The distinction at  $\text{LWP} = 100\text{ g m}^{-2}$  is very similar to the distinction at  $\tau = 15$ . There are fewer clouds with  $\text{LWP} > 100\text{ g m}^{-2}$  than with  $\tau > 15$ , which reduces the scatter for cases with  $\text{LWP} > 100\text{ g m}^{-2}$ . The difference in correlation coefficient and in slope is enhanced if divided at  $\text{LWP} = 100\text{ g m}^{-2}$  as compared to dividing the data at  $\tau = 15$ . The slope deviates more from the slope of an adiabatic cloud in the cases of smaller LWP than in the cases with  $\tau < 15$ .

What causes the differences in correlation and slope between  $\tau$  and  $r_e$ ? Nakajima and Nakajima [1995] suggested the onset of precipitation in thick clouds to cause the negative correlation between  $r_e$  and  $\tau$ . Based on ECHAM results grouped into precipitating and non-precipitating clouds we confirm the above hypothesis as shown in Figure 2. The correlation coefficient is slightly positive for non-precipitating clouds, and negative for precipitating clouds. The sample sizes produced by this categorization are very different as

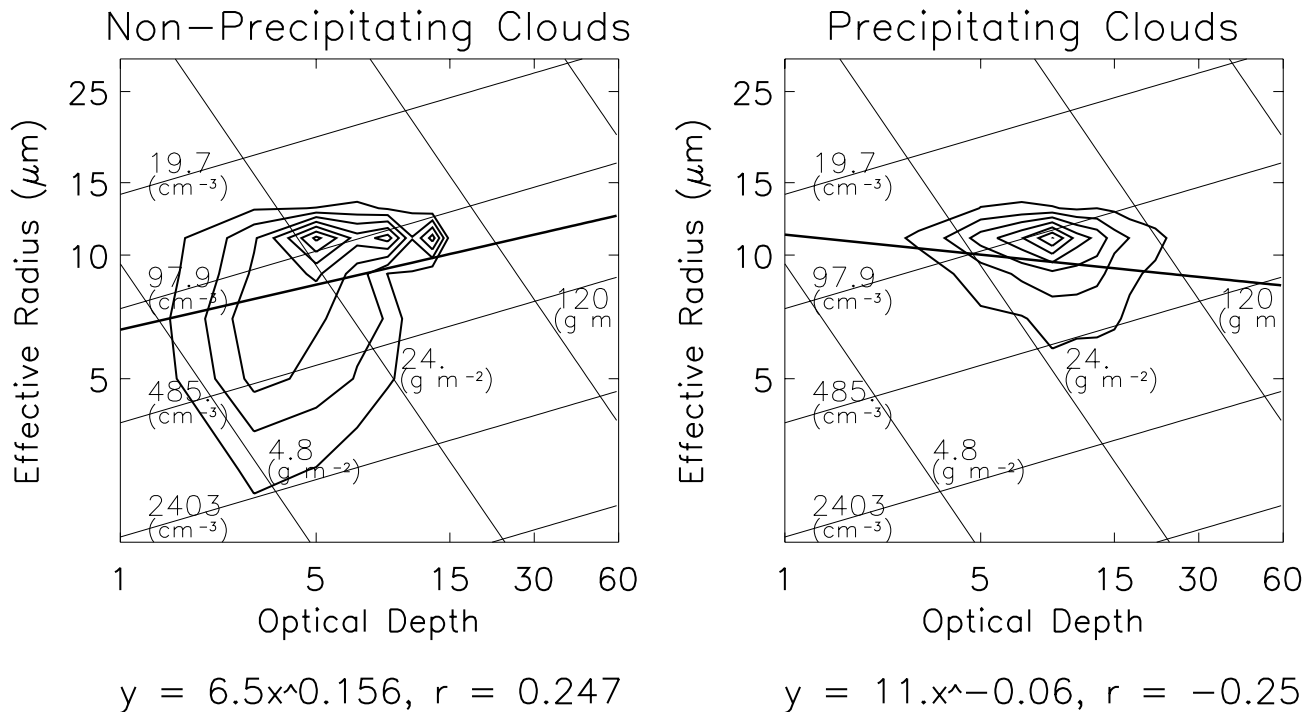


**Figure 2.** As figure 1, but for non-precipitating clouds(left) and precipitating clouds (right).

compared to the distinction in optical depth. Two thirds of the clouds precipitate, whereas only 20% of the clouds have  $\tau > 15$ . Of the precipitating clouds,  $\tau$  ranges between 4 and 25, i. e. spans a larger range than in case of optically thick clouds. The correlation coefficients are very similar for precipitating clouds and optically thick clouds, but the slope is smaller for precipitating clouds, which is caused by the different range of  $\tau$  encompassed.

The non-precipitating clouds are more positively correlated than the clouds with  $\tau < 15$ , and the slope of 0.16 is closer to that expected for an adiabatic cloud than the slope of 0.13 for optically thin clouds. However, a slope of 0.15 can also be obtained if the threshold in optical depth is lowered to 10 (not shown), because then fewer clouds start to precipitate.

Another cause for the opposite correlation between  $\tau$  and  $r_e$  might be that optically thin clouds are often single-layer clouds and thicker ones extend over many layers. If multi-layer clouds are separated by a cloud-free layer, then the effective radius obtained from cloud top cannot be expected to be correlated to the optical depth of all the cloud layers [e.g. *Schueller, 1999*]. However, as shown in Figure 3, in ECHAM the slope is more positive in the multi layer case than in the single layer case. Likewise, the correlation coefficient is negative in the single layer case and close to zero in the multi layer case. The slope and correlation coefficients of single layer clouds can be increased if only clouds which have a partial cloud cover of  $> 0.9$  are included (not shown).

## Discussion and conclusions

The ECHAM GCM was used to explain the difference in the relationship between cloud optical thickness and effective radius which occurs for marine clouds at  $\tau = 15$  in a region off the coast of California where probability den-

sity functions of  $\tau$  and  $r_e$  were studied using AVHRR data [*Austin et al., 1999*]. However, the same conclusions can be drawn if the analysis is applied globally (not shown). The difference in relationship is also seen if  $\tau = 10$  or  $\tau = 20$  are chosen as a separator. It is even more pronounced for  $\tau = 10$ , because in clouds with  $\tau < 10$  precipitation formation occurs less often and they are more often comprised of single layer clouds only. Likewise the difference in slope and correlation is less pronounced if  $\tau = 20$  is used as a discriminator. Analyses of the ECHAM grid cells off the coast of California showed that this distinction is strongly related to the onset in precipitation, when the clouds become non-adiabatic and  $N_l$  changes but cannot be explained in terms of single layer versus multi layer clouds. With this conclusion the present study gives the most likely answer as to why the satellite detects the different correlation regimes.

What is it in particular that precipitation does to the  $\tau$ - $r_e$  relationship? Precipitation processes in the model, as in the real world, work in the direction of keeping LWP constant, since the thicker the cloud the more water is removed from it through rain. Therefore, precipitation in the model reduces the range of variation of LWP (Figure 2) more so than the range of variation of  $N_l$ . The reduction in the range of variation in LWP makes the influences of large  $N_l$  variations on  $\tau$  (i. e. the indirect aerosol albedo effect) easier to detect, since it makes more prominent cloud ensembles in which LWP is near-constant and  $r_e$  decreases as LWP increases. Non-precipitating clouds in ECHAM, on the other hand, seem to be fairly close to being adiabatic and, thus, show on average a  $r_e \sim \tau^{1/6}$  slope.

Clearly, more studies are needed to explain in detail why the satellite is only able to observe an indirect cloud albedo effect for optically thick clouds. Also, other causes for deviations from an adiabatic LWP such as mixing with cloud-free air due to turbulent and organized entrainment were

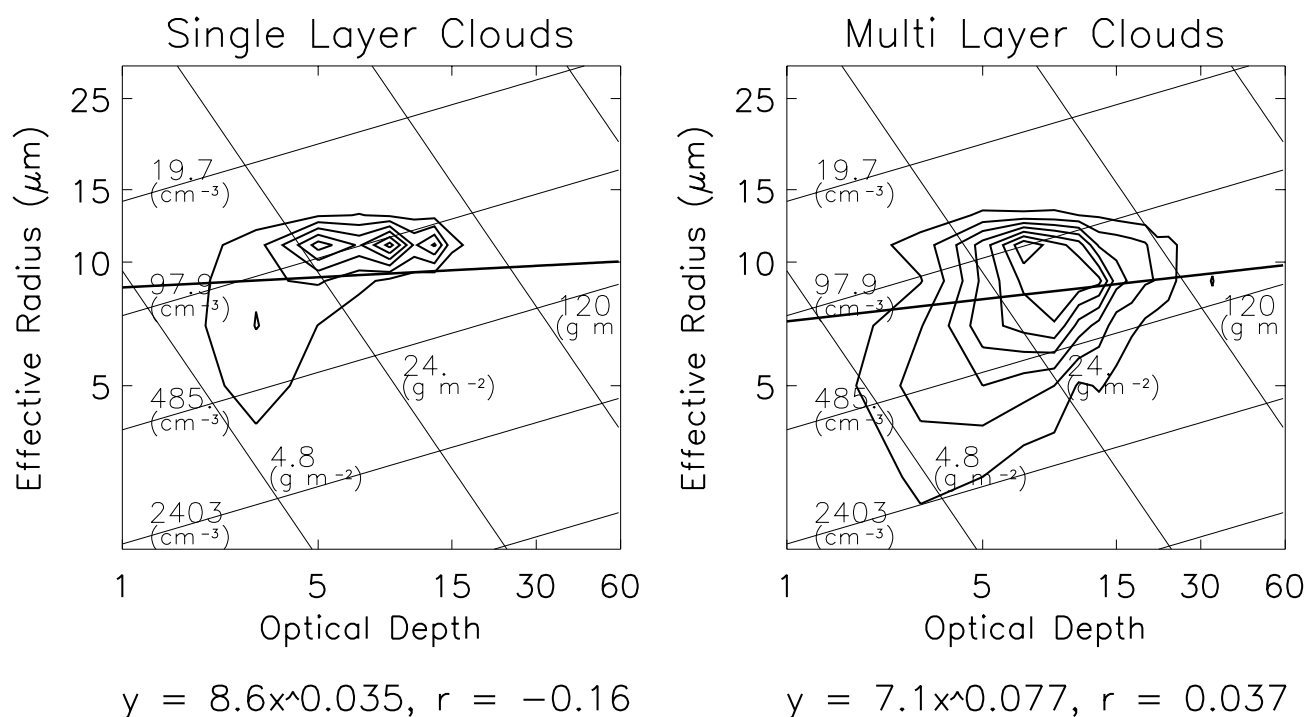


**Figure 3.** As figure 1, but for clouds consisting of a single layer(left) and those consisting of multiple layers (right).

neglected as they are thought to be of smaller importance than the onset of precipitation, but are likely to explain deviations from an adiabatic LWP in nature.

**Acknowledgments.** We thank Anthony DelGenio and the reviewers for helpful comments and suggestions. Ulrike Lohmann thanks Petro Canada for support.

## References

- Austin, P. H., M. Szczodrak, and G. M. Lewis, Spatial variability of satellite-retrieved optical depth and effective radius in marine stratocumulus clouds, in *Proceedings of the 10th Conference on Atmospheric Radiation*, pp. 237–240, Madison, Wisconsin, Amer. Meteorol. Soc., 1999.
- Boucher, O., and U. Lohmann, The sulfate-CCN-cloud albedo effect: A sensitivity study with two general circulation models, *Tellus, Ser. B*, **47**, 281–300, 1995.
- Brenguier, J.-L., et al., Radiative properties of boundary layer clouds: Optical thickness and effective radius versus geometric thickness and number concentration, *J. Atmos. Sci.*, 2000, in press.
- Brenguier, J.-L., H. Pawlowska, L. Schüller, R. Preusker, J. Fischer, and Y. Fouquart, An overview of the ACE-2 CLOUDY-COLUMN closure experiment, *Tellus*, 1999, subm. to.
- Han, Q., W. B. Rossow, J. Chou, and R. Welch, Global survey of the relationship of cloud albedo and liquid water path with droplet size using ISCCP, *J. Clim.*, **11**, 1516–1528, 1998.
- Jones, A., D. L. Roberts, and A. Slingo, A climate model study of indirect radiative forcing by anthropogenic sulphate aerosols, *Nature*, **370**, 450–453, 1994.
- King, M. D., Radiative properties of clouds, in *Aerosol-Cloud-Climate Interactions*, edited by P. V. Hobbs, vol. 54, pp. 123–149, Academic, 1993.
- Leaith, W., G. A. Isaac, J. W. Strapp, C. M. Banic, and H. A. Wiebe, The relationship between cloud droplet number concentrations and anthropogenic pollution: Observations and climatic implications, *J. Geophys. Res.*, **97**, 2463–2474, 1992.
- Lohmann, U., J. Feichter, C. C. Chuang, and J. E. Penner, Predicting the number of cloud droplets in the ECHAM GCM, *J. Geophys. Res.*, **104**, 9169–9198, 1999.
- Nakajima, T., and T. Nakajima, Wide-area determination of cloud microphysical properties from NOAA AVHRR measurements for FIRE and ASTEX regions, *J. Atmos. Sci.*, **52**, 4043–4059, 1995.
- Nakajima, T., M. King, J. Spinhirne, and L. Radke, Determination of the optical thickness and effective particle radius of clouds from reflected radiation measurements. Part II: Marine stratocumulus observations, *J. Atmos. Sci.*, **48**, 728–750, 1991.
- Rockel, B., E. Raschke, and B. Weyres, A parameterization of broad band radiative transfer properties of water, ice and mixed clouds, *Beitr. Phys. Atmos.*, **64**, 1–12, 1991.
- Schüller, L., Fernerkundung von klimarelevanten Wolkeigenschaften mit satelliten- und flugzeuggestützten Radiometern, Ph.D. Thesis, Free University of Berlin, 1999.
- Ulrike Lohmann and Chris Tyler, Atmospheric Science Program, Dept. of Physics, Dalhousie University, Halifax, N.S. B3H 3J5, Canada, (e-mail: Ulrike.Lohmann@Dal.Ca)
- George Tselioudis, NASA/GISS, Columbia University, 2880 Broadway, New York, N.Y. 10025, U.S.A.

(Received September 25, 1999; revised February 17, 2000; accepted February 21, 2000.)